Limit state assessment of nodal zone capacity in strut-and-tie models

Tjen N. Tjhin[†]

Buckland & Taylor Ltd., North Vancouver, British Columbia, Canada

Daniel A. Kuchma[‡]

*Department of Civil and Environmental Engineering,
University of Illinois at Urbana-Champaign, Urbana, Illinois, USA*

Abstract. A method based on the lower-bound theorem of limit analysis is presented for the capacity assessment of nodal zones in strut-and-tie models. The idealized geometry of the nodal zones is formed by the intersection of effective widths of the framing struts and ties. The stress distribution is estimated by dividing the nodal zones into constant stress triangles separated by lines of stress discontinuity. The strength adequacy is verified by comparing the biaxial stress field in each triangle with the corresponding failure criteria. The approach has been implemented in a computer-based strut-and-tie tool called CAST (Computer-Aided Strut-and-Tie). An application example is also presented to illustrate the approach.

Keywords : computer aided design; interactive graphics; concrete; struts; ties; limit analysis

1. Introduction

The Strut-and-Tie Method (STM) (e.g. Marti 1985, Schlaich, *et al.* 1987) is a lower bound limit analysis and design method of D-(Discontinuity) regions in structural concrete. In the STM, an internal truss is idealized in the cracked body of concrete to carry the loading through the D-region to its supports or boundaries, representing an idealized flow of forces or internal load-carrying system of the D-region at the ultimate limit state. Referred to as strut-and-tie model, this truss consists of struts, ties, and nodes, where struts are the compression members, ties are the tension members, and nodes, also known as nodal zones or nodal regions, are the meeting regions of the struts and ties (Fig. 1).

Depending on the types of forces being connected, there are four basic types of nodes, namely CCC, CCT, CTT, and TTT, as illustrated in Fig. 2, where F_c and F_t in the figure denote strut and tie forces, respectively. Originally used for nodes with three members framing, for discussion purposes herein, the terms CCC, CCT, CTT, and TTT can be extended to include nodes with more than three framing members as follows: CCC nodes are those in which all the framing members are struts, CCT nodes are those in which one of the framing members is a tie, CTT nodes are those in which

† Structural Engineer, Corresponding Author, E-mail: tjhin@illinoisalumni.org
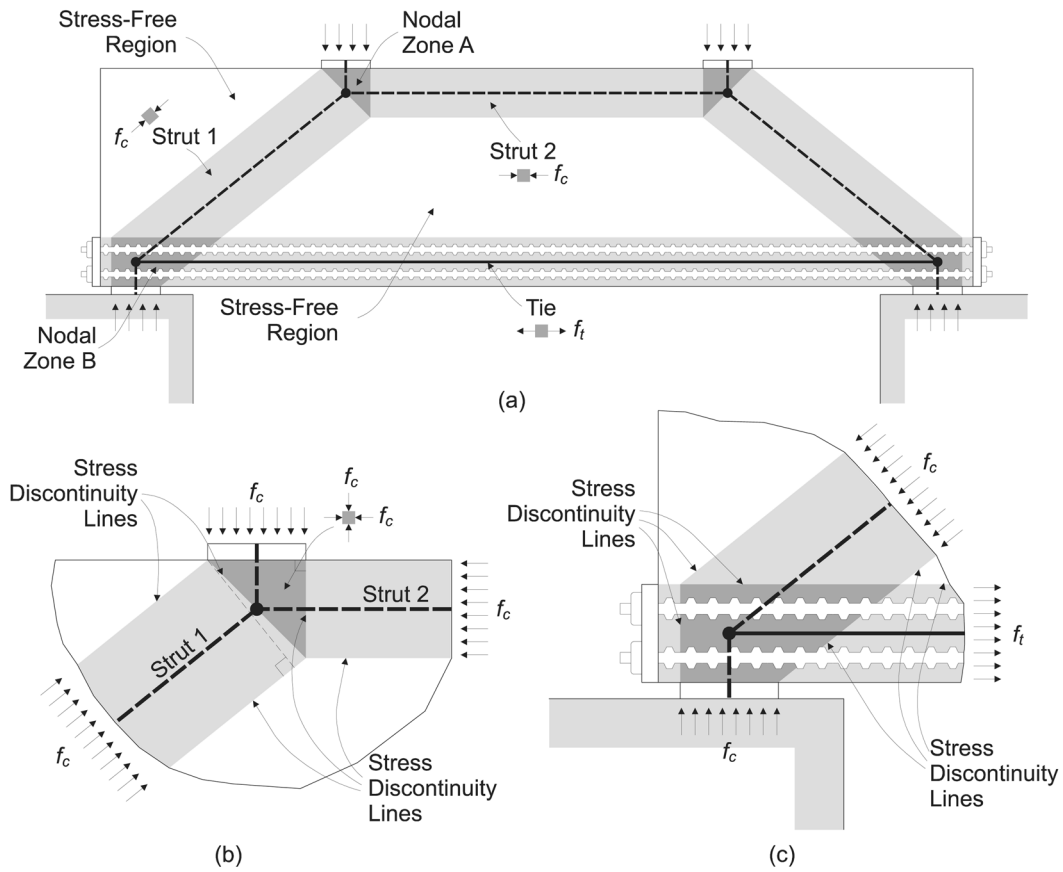‡ Associate Professor, E-mail: kuchma@uiuc.edu

Fig. 1 A deep beam under two point loads: (a) Selected strut-and-tie model (b) Nodal zone *A* (c) Nodal zone *B*
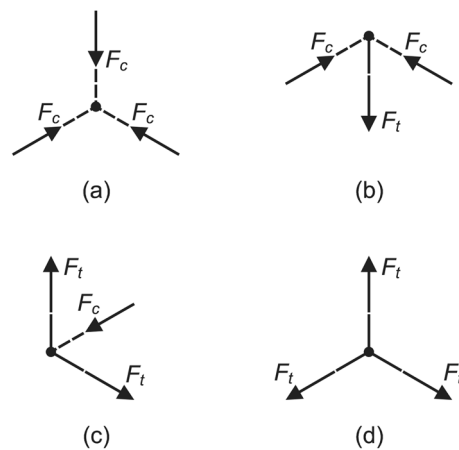

Fig. 2 Basic node types: (a) CCC (b) CCT (c) CTT (d) TTT

two or more of the framing members are ties, and TTT nodes are those in which all the framing members are ties.
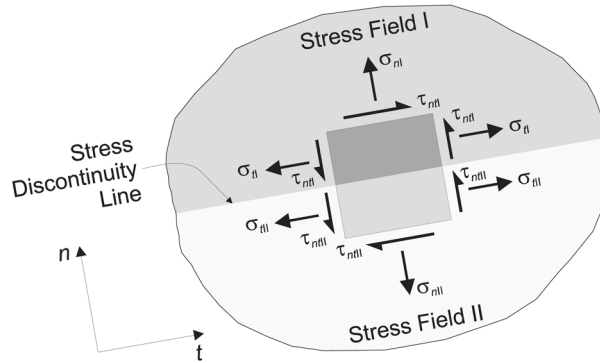
Fig. 3 State of stress along a line of stress discontinuity between two stress fields I and II

In limit analysis term, a strut-and-tie model is a statically admissible stress field system of a lower-bound solution. The stress fields in struts and ties are uniaxial and are usually assumed to be uniformly distributed across the effective widths. The stress fields in nodal zones are biaxial and triaxial for 2-D and 3-D strut-and-tie models, respectively. The strength adequacy of these stress fields is checked against the corresponding failure criteria. Because of the different types of stress fields, stress discontinuities (e.g. Chen and Han 1988, Nielsen 1999) exist at the interface between the strut and node stress fields and between the tie and node stress fields, as shown in Figs. 1(b) and (c). As indicated in the same figures, stress discontinuities also occur along the longitudinal boundaries of strut or tie stress fields if the selected stress distribution across the strut and tie effective widths is uniform. With reference to Fig. 3, equilibrium of a statically admissible stress field system requires that

$$\sigma_{nI} = \sigma_{nII} \tag{1}$$

and

$$\tau_{ntI} = \tau_{ntII} \tag{2}$$

at every point along the line of stress discontinuity between two stress fields I and II.

The distribution of node stress fields depends on the idealized shape, which in turn depends on the effective width and direction of the strut or tie stress fields entering the node. The simplest idealized shape of a nodal zone is one which is formed by the intersection of effective widths of struts and ties whose centerlines coincide at the node. An example of this construction is shown in Fig. 4(b) for a nodal zone with four struts intersecting (Fig. 4(a)). This shape is simple to construct, but the resulting state of stress is typically complex and thus difficult to determine. Finite element analyses have been used to estimate the stress distribution in this type of nodal zones (Fig. 5) (e.g. Alshegeir and Ramirez 1992, Yun and Ramirez 1996). Despite providing valid stress distribution, these analyses require consideration of strain compatibility.

Variants of nodal zone shape construction techniques have been proposed to simplify the stress distribution in nodal zones. These include the classical hydrostatic approach (Fig. 4(c)) (e.g. Marti 1985 and Nielsen 1999) and modified hydrostatic approach (Fig. 4(d)) (Schlaich and Anagnostou 1990).

In the hydrostatic approach, the idealized shape of nodal zones is arranged such that the stresses on all nodal zone sides, from the truss member forces as well as from the boundary forces meeting
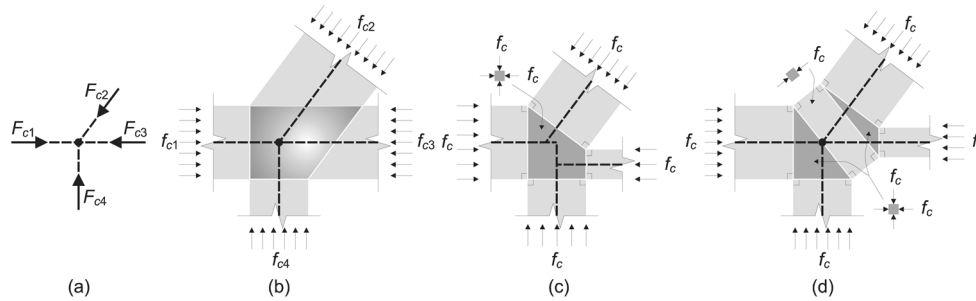
Fig. 4 Examples of shape idealization of a nodal zone with four struts intersecting: (a) Forces acting on the node (b) Simple shape (c) Hydrostatic shape (d) Modified hydrostatic shape
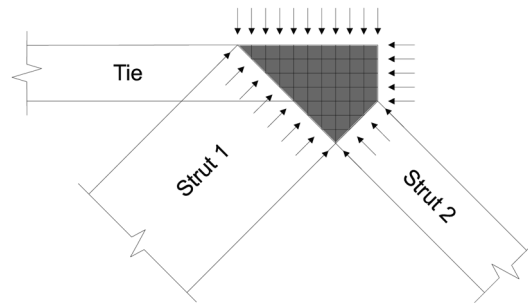

Fig. 5 Example of a finite element model used to obtain the stress distribution in a CCT nodal region (Adapted from Yun and Ramirez 1996)

at the nodes, are equal. This shape drastically simplifies the state of stress inside the nodes to be hydrostatic, i.e., the stresses are isotropic, uniform, and equal to those on the sides. However, laying out nodal zones in this manner can be very laborious for nodes bounded by more than three truss members (Fig. 4(a)) as the centerlines of truss members framing into hydrostatic nodes of more than three sides are unlikely to coincide (Fig. 4(c)). In addition, the truss and the dimensions of the struts and ties have to be drawn to scale to establish the geometry of the nodal zones. As a result, several iterations in determining the forces due to the change in truss geometry are needed.

The modified hydrostatic approach was developed to overcome the difficulty in constructing hydrostatic nodes with more than three members intersecting. It utilizes the hydrostatic node rules, except that nodes with more than three members intersecting are handled by dividing them into several hydrostatic nodes of triangular shapes connected by short prismatic struts. Fig. 4(d) shows how the CCC node of Fig. 4(a) is arranged using this approach.

This paper presents an analytical approach for assessing the capacity of nodal zones with the geometry formed by intersections of the effective widths of the framing struts or ties. The stress distribution in the nodes is evaluated solely based on equilibrium – through construction of discontinuous stress fields. In addition to the formulation used in this approach, the implementation and example application are briefly presented. More description of the approach is provided in Tjhin (2004).

2. Formulation

2.1. Idealized stress distribution

2.1.1. Nodal zones with three sides

The state of stress of node zones having triangular shapes and subjected to uniform tractions on the sides is constant, thus the term constant stress triangles. An example of these nodal zones is the CCC node shown in Fig. 6(a). The resulting biaxial stress distribution in the nodal zone, i.e., the triangle *ABC* of Fig. 6(b), is uniform and can be presented in the form of Szmodits' Mohr's circle, as illustrated in Fig. 6(c).

In general, the stresses in a constant stress triangle shown in Fig. 7 can be expressed by the following equations:

$$\sigma_x = \frac{F_{2x}a_{1x} - F_{1x}a_{2x}}{(a_{1x}a_{2y} - a_{1y}a_{2x})t} \tag{3}$$

$$\sigma_y = \frac{F_{2y}a_{1y} - F_{1y}a_{2y}}{(a_{1x}a_{2y} - a_{1y}a_{2x})t} \tag{4}$$

$$\tau_{xy} = -\tau_{yx} = \frac{F_{2x}a_{1y} - F_{1x}a_y}{(a_{1x}a_{2y} - a_{1y}a_{2x})t} \tag{5}$$
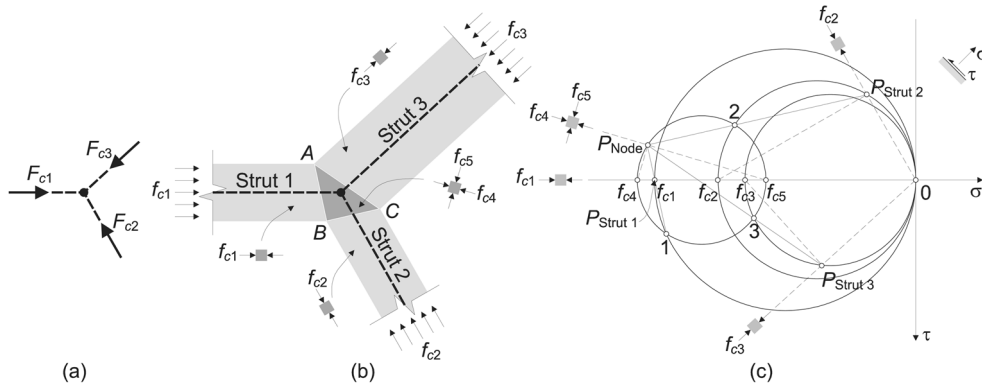

Fig. 6 Example of a CCC node having three members meeting: (a) Forces acting on the node (b) Simple nodal region shape and the stress state (c) Mohr's circle describing biaxial stresses in the nodal zone
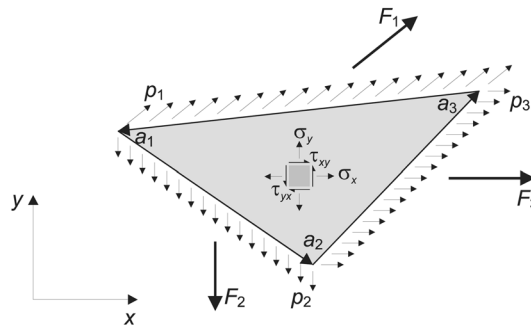

Fig. 7 Constant stress triangle

where σ_x = normal stress parallel to x axis, σ_y = normal stress parallel to y axis; τ_{xy} = shear stress acting on the plane normal to y axis in the direction of x axis; τ_{yx} = shear stress acting on the plane normal to x axis in the direction of y axis; F_1, F_2, F_3 = strut or tie force demands acting on triangle sides 1, 2, and 3, respectively; F_1, F_2, F_3 = vectors of strut or tie force demands acting on nodal zone sides 1, 2, and 3, respectively; F_{1x}, F_{1y} = components of F_1 in x and y directions, respectively; F_{2x}, F_{2y} = components of F_2 in x and y directions, respectively; a_1, a_2, a_3 = lengths of triangle sides 1, 2, and 3, respectively; a_1, a_2, a_3 = vectors of triangle sides 1, 2, and 3, respectively; a_{1x}, a_{1y} = components of a_1 in x and y directions, respectively; a_{2x}, a_{2y} = components of a_2 in x and y directions, respectively; p_1, p_2, p_3 = $F_1/(a_1t)$, $F_2/(a_2t)$, $F_3/(a_3t)$ = tractions acting on triangle sides 1, 2, and 3, respectively; p_1, p_2, p_3 = traction vectors acting on nodal zone sides 1, 2, and 3, respectively. It should be noted that the traction, p, is not generally the same as strut stress demand, f_c, nor equivalent tie stress demand, f_t.

2.1.2. Nodal zones with more than three sides

Stress conditions of nodal zones consisting of more than three sides can be obtained by dividing them into several constant stress triangles. The triangles are separated by lines of stress discontinuity and are arranged such that the state of stress in all triangles is constant and equilibrium along the lines of stress discontinuity is satisfied. The lines of stress discontinuity must be introduced at the vertices of the nodal zones to achieve these conditions. This procedure is valid according to the STM because equilibrium at each point in the triangles and at the lines of stress discontinuity is satisfied. Fig. 8 shows how this approach is applied to the nodal zone of Fig. 4(b).

For nodal zones with even number of sides, the minimum number of triangles necessary to achieve equilibrium conditions, n_t, is

$$n_t = 2n_s - 4 \tag{6}$$

where n_s = number of nodal zone sides (larger than or equal to 3). For nodal zones having odd number of sides,

$$n_t = 2n_s - 5 \tag{7}$$

Examples of nodal zones with even and odd number of sides are provided in Figs. 9(a) and (b),
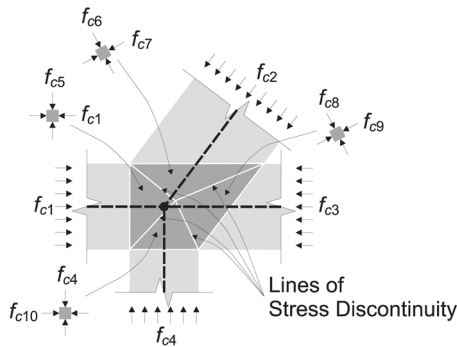

Fig. 8 Nodal zone of Fig. 4 constructed according to the proposed node dimensioning
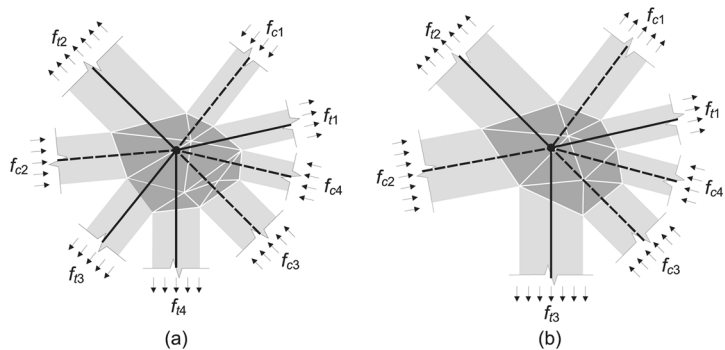

Fig. 9 Examples of nodal zones divided into constant stress triangles: (a) Eight-side nodal zone (b) Seven-side nodal zone
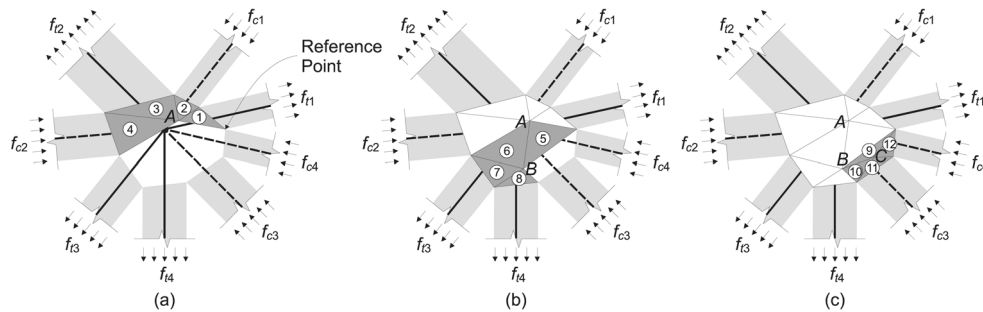
Fig. 10 Construction of constant stress triangles for nodal zone of Fig. 9(a): (a) Triangles 1 to 4 (b) Triangles 5 to 8 (c) Triangles 9 to 12

respectively. It is worth noting that the use of minimum number of constant stress triangles works well if the stresses acting on the nodal zone sides are of the same order of intensity. This requirement is easily satisfied as the stresses in struts and the equivalent stresses in ties are normally aimed to be of the same order in design.

A step-by-step process similar to the procedure of constructing discontinuous stress fields by Hajdin (1990) is used for constructing constant stress triangles. In each step, four triangles are built, and the common vertex of triangles in the nodal zone is determined. Examples of how this process is done are shown in Fig. 10 for the nodal zone of Fig. 9(a). The position of the common vertex of triangles in the nodal zone (Points *A*, *B*, and *C* in Fig. 10) is established by considering the equilibrium in *x* and *y* directions, moment equilibrium about axis perpendicular to the nodal zone plane, and criteria for discontinuity lines (Eqs. (1) and (2)).

2.1.3. Treatments of tie forces and body forces

Two assumptions can be employed in nodal zones with framing ties, as can be found in CCT, CTT, and TTT nodes. Traditionally adopted in nodal zone capacity assessment, the first assumption assumes tie forces are anchored by fictitious bearing plates behind the node (Fig. 11(a)). With this assumption, the nodes can essentially be treated as CCC nodes; the nodal zone stresses are resisted
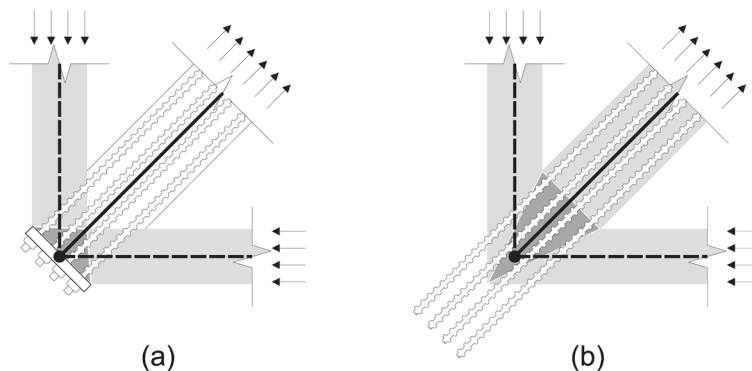

Fig. 11 Two treatments of steel reinforcement in CCT, CTT, and TTT nodes: (a) Anchored by fictitious bearing plates behind the node (b) evenly distributed and extend inside and beyond the nodal zones
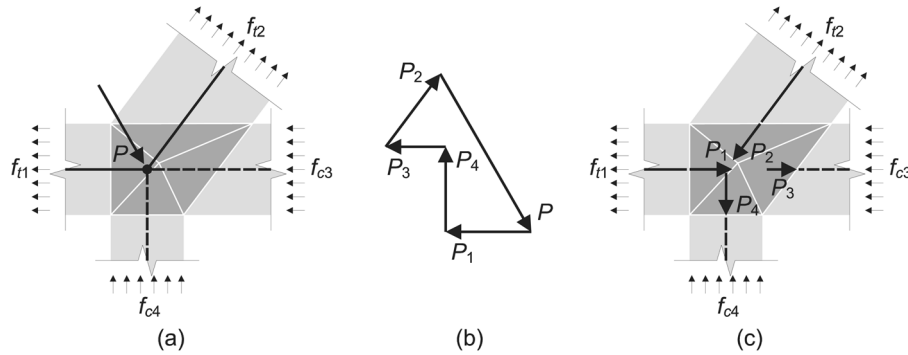
Fig. 12 Example of how a body force acting on a node is treated in the proposed node dimensioning: (a) Nodal zone (b) Decomposition of the body force according to the head-to-tail rule (c) Statically equivalent forces acting on the sides of the node

by the concrete alone. The second treatment assumes the tie steel extends inside and beyond the nodal zones (Fig. 11(b)). In addition, the steel is assumed to be evenly distributed in the nodal zones, i.e., smeared steel is assumed. With this assumption, the stresses in the nodes are shared between concrete and steel, but the bearing stress effects due to tie anchorages are ignored. Even though the second assumption is used throughout this paper, the use of constant stress triangles is also applicable for the first assumption.

Any body forces acting on nodal zones are treated as if the force components acted on the sides of the nodal zones. An example of how this is done is illustrated in Fig. 12. With this assumption, a body force that acts on a node will not have direct influence on the stress distribution in the nodal zone itself, but it will affect the stress distribution in all other nodal zones and in all of the struts and ties. The assumption that body forces have no direct influence on the stress distribution of nodal zones carrying them can be justified by the fact that body forces mostly come from conservative lumping of self-weight or from indirect supports, i.e., reaction forces of other members framing into and forming integral parts with the D-region under consideration.

2.2. Capacity assessment

The strength adequacy of nodal zones is verified by comparing the stresses in each constant stress triangle with the corresponding biaxial stress failure criteria. In checking the adequacy of the constant stress triangles of CCC nodes, the modified Mohr-Coulomb yield criterion according to Chen and Drucker (1969) (Fig. 13) provides a representation of the response of planar nodal zones subjected to biaxial compressive stresses. In the figure, f_{cr} = cracking strength of concrete, and $f_{cu} = v f'_c$ = effective compressive stress capacity of nodes, f'_c = specified concrete compressive strength, and v = effectiveness factor. The effectiveness factor is applied to the failure criterion to account for factors influencing the strength of nodal zones, such as level of transverse straining as well as the volume and condition of surrounding concrete. This use of effectiveness factors for assessing nodal zone strength is consistent with the standard code approach for evaluating strengths of struts and reinforcement quantities of ties. The reinforcing steel of the ties framing into the nodal zones is assumed to have no contribution in carrying the compressive stresses. A dimensionless parameter termed stress ratio can be introduced as a quantitative measure or the strength adequacy.
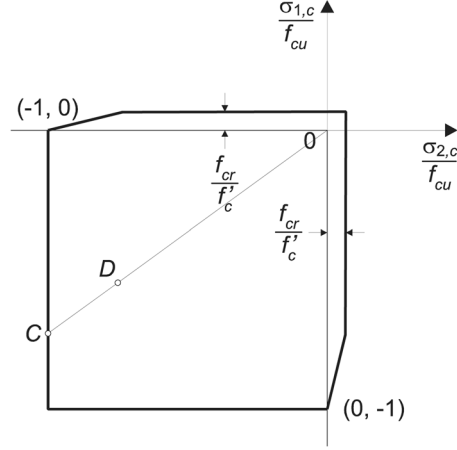
Fig. 13 Concrete failure criteria used for the stress check of CCC nodes in the proposed method

This stress ratio is graphically represented by the ratio of line segments *OD* to *OC* in Fig. 13, where *D* is the demand point and *C* is the capacity point. A stress ratio greater than 1.0 indicates an overstress.

The introduction of effectiveness factors to the selected failure criterion is certainly a simplification of the actual response of concrete material as they have to absorb effects causing deviation from the idealized response. However, it is justified by the fact that the interest is in the concrete of the nodal zones, not in the strength of the virgin material. Although more are needed, experimental programs to propose or validate effectiveness factors appropriate to stress state of nodal zones have been conducted (e.g. Bergmeister, *et al*. 1991, Thompson, *et al*. 2005, Thompson, *et al*. 2006).

In checking the strength adequacy of the constant stress triangles of CCT, CTT, and TTT nodes, the stress distribution between the concrete and steel (Fig. 14) follows the equilibrium equations derived by Müller (1978) as follows:
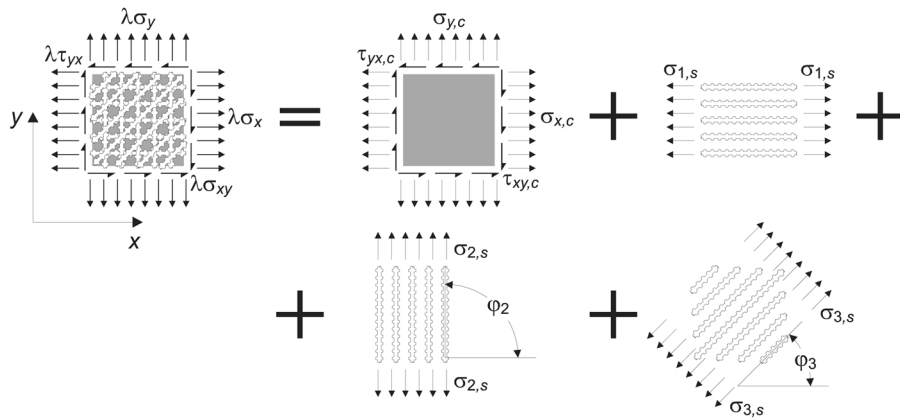

Fig. 14 Example of stress distribution between concrete and steel reinforcement of a unit nodal zone element with three directions of reinforcement

$$\lambda\sigma_x - \sigma_{x,c} - \sum_{i=1}^{n} \sigma_{i,s}\cos^2\varphi_i = 0 \tag{8}$$

$$\lambda\sigma_y - \sigma_{y,c} - \sum_{i=1}^{n} \sigma_{i,s}\sin^2\varphi_i = 0 \tag{9}$$

$$\lambda\tau_{xy} - \tau_{xy,c} - \sum_{i=1}^{n} \sigma_{i,s}\sin\varphi_i\cos\varphi_i = 0 \tag{10}$$

where λ = dimensionless factor extrapolating the stress demand to the stress capacity, $\sigma_{x,c}$ = x-direction mal stress carried by concrete, $\sigma_{y,c}$ = y-direction normal stress carried by concrete, $\tau_{xy,c} = -\tau_{yx,c}$ x-y direction shear stress carried by concrete, $\sigma_{i,s}$ = stress carried by i-direction steel reinforcement, φ_i = angle of i-direction steel reinforcement with respect to positive x axis, and n = number of steel directions framing into the nodal zone.

A linearized version of the Mohr-Coulomb yield criterion (Hajdin 1990) graphically represented by Fig. 15 is used for checking the adequacy of constant stress triangles of CCT, CTT, and TTT nodes. The elasto-plastic yield condition is used for the reinforcing steel in tension.

Because the parameter λ in Eqs. (8)-(10) represents the ratio of capacity point to demand point, the equivalent stress ratio for CCT, CTT, and TTT nodes is the inverse of λ, i.e.,

$$\text{Stress Ratio} = \frac{1}{\lambda} \tag{11}$$

The value of λ is obtained by maximizing λ subject to equality constraints of Eqs. (8)-(10) and inequality constraints of inequalities represented by Fig. 15 using simplex method in linear programming (e.g. Hadley 1962). For cases in which the concrete governs the capacity, the stress ratio is graphically represented by the ratio of line segments OD to OC in Fig. 15, where D is the demand point and C is the capacity point.
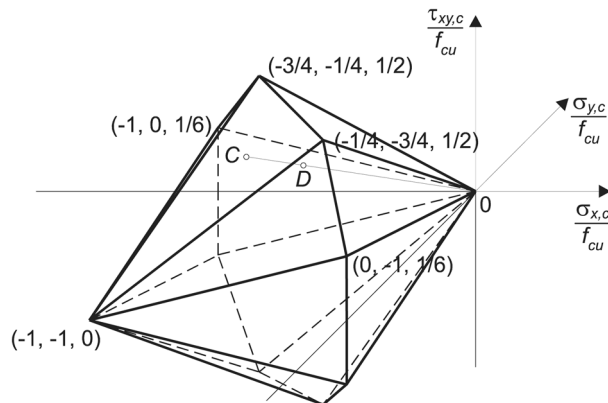

Fig. 15 Concrete failure criteria used for the stress check of CCT and TTT nodes in the proposed method (Adapted from Hajdin 1990)

3. Implementation

The approach discussed above has been implemented in CAST (Computer Aided Strut-and-Tie) Analysis and Design Tool (Tjhin and Kuchma 2004), a special-purpose computer application for analysis and design of structural concrete based on the STM (Tjhin and Kuchma 2007).

In CAST, the geometry of nodal zones is automatically generated during the dimensioning of struts and ties framing into the nodes. Once a strut-and-tie model and dimensions of struts and ties are available, CAST computes the tractions acting on nodal zones based on the framing strut and tie forces, divides the nodal zones into constant stress triangles, computes the stress demands in the triangles, computes the corresponding stress capacities, and computes the corresponding stress ratios.

4. Application example

An application of the method is now illustrated for two nodal zones B and F of the selected strut-and-tie model of a propped cantilever deep beam with an opening shown in Fig. 16. The out-of plane dimension of the beam is 600 mm. A compressive strength of concrete, f'_c of 30 MPa and the
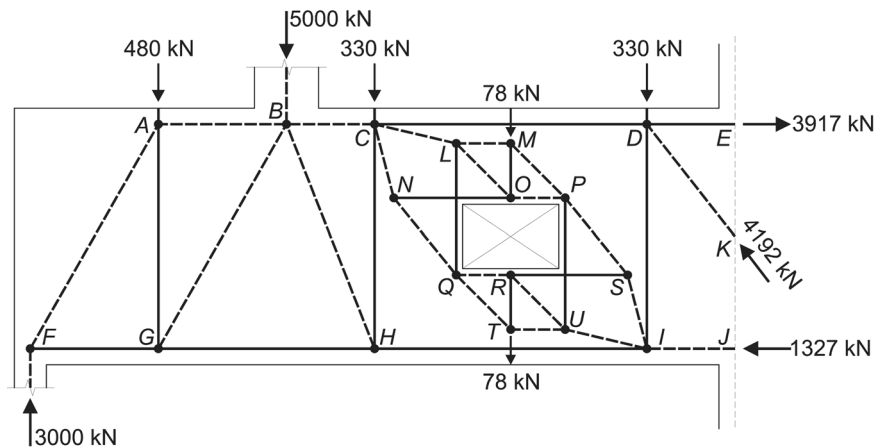

Fig. 16 Geometry and selected strut-and-tie model of the design example

Table 1 Stress demands of nodal zone B

Triangle ID	x-y-Direction Stress			Principal Stress		
	x-Dir. (MPa)	y-Dir. (MPa)	Shear (MPa)	Max. (MPa)	Min. (MPa)	Principal Dir. (degrees)
1	-7.29	-9.45	-0.49	-7.19	-9.55	-12.15
2	-7.08	-8.33	0	-7.08	-8.33	0
3	-5.78	-7.92	-0.73	-5.56	-8.15	-17.12
4	-3.77	-7.92	-0.61	-3.68	-8.01	-8.21
5	-4.22	-9.19	-1.37	-3.87	-9.54	-14.42

yield strength of the steel reinforcement, f_y, of 420 MPa are used. The struts and ties were designed using CAST. The nodes were also designed using CAST according to the method described in this paper.

The effectiveness and strength reduction factors should be ideally selected according to the governing design code. A stress limit, $f_{cu} = vf'_c$, equal to $0.6f'_c$ was used for dimensioning struts and nodes. A strength reduction factor, ϕ, of 0.75 was applied to all struts, ties, and nodes to account for variations in construction quality. These values are selected to be reasonably consistent with the strut-and-tie design provisions per ACI Building Code Requirements for Structural Concrete (ACI 318-05).

Nodal zone *B* is a 5-sided CCC node. Therefore, the nodal zone is divided into 2(5)–5=5 constant stress triangles according to Eq. (7) and is checked for its strength adequacy according to the modified Mohr-Coulomb yield condition of Fig. 13. Fig. 17(a) shows the geometry, numbering, principal stress directions, and stress ratios of the triangles. Table 1 presents the triangle biaxial stress demands described in both the *x-y* coordinate system and principal directions. A positive
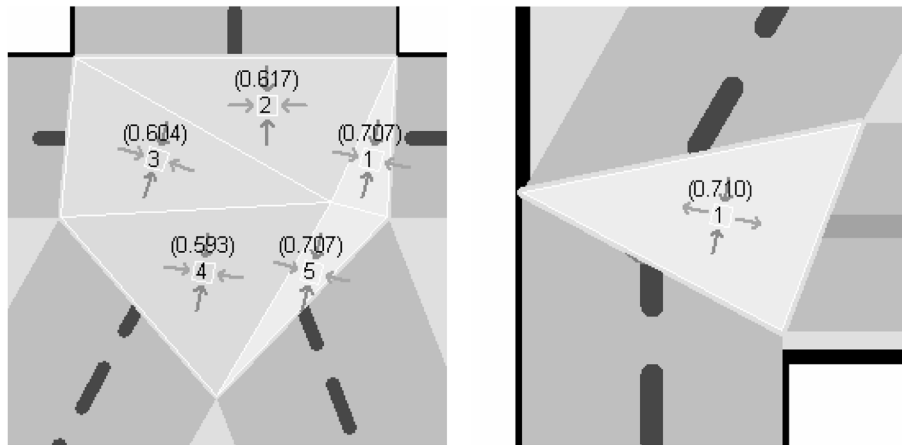

Fig. 17 Geometry, principal stress directions, and stress ratios of constant stress triangles of: (a) Nodal zone *B* (b) Nodal zone *F*
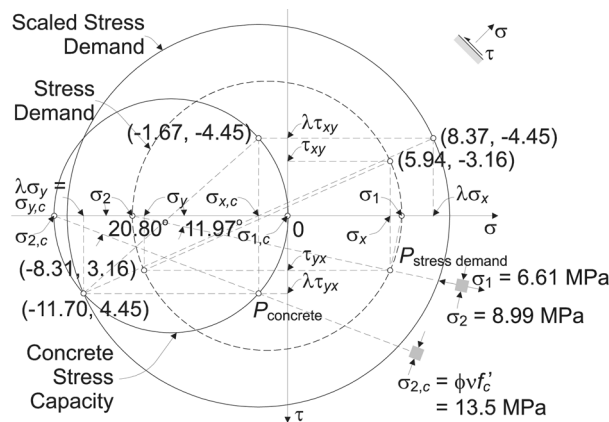

Fig. 18 Mohr's circle representation of the stress state of nodal zone *F*

Table 2 Concrete biaxial stress demands, capacities, and stress ratios of constant stress triangles of nodal zone *B*

Triangle ID	Concrete Stress Demand (MPa)			Concrete Stress Capacity (MPa)			Stress Ratio
	x-Dir.	*y*-Dir.	Shear	*x*-Dir.	*y*-Dir.	Shear	
1	-7.29	-9.45	-0.49	-10.31	-13.35	-0.68	0.71
2	-7.08	-8.33	0	-11.47	-13.50	0	0.62
3	-5.78	-7.92	-0.73	-9.58	-13.13	-1.21	0.60
4	-3.77	-7.92	-0.61	-6.35	-13.35	-1.03	0.59
5	-4.22	-9.19	-1.37	-5.97	-13.00	-1.94	0.71

normal stress value indicates tension, and a negative value denotes compression. The sign convention of shear stress is shown in Fig. 18. Table 2 lists the concrete contribution in carrying the biaxial stress demands, the available biaxial stress capacities, and the corresponding stress ratios.

Nodal zone *F* is a 3-sided CCT node. Thus, it is a constant stress triangle. Fig. 17(b) shows the geometry, numbering, principal stress directions, and stress ratios of the triangle. Fig. 18 shows a Mohr's circle representation of the stress state of nodal zone *F*, compactly representing the stress demand, concrete contribution in carrying the biaxial stress demand, and the available stress capacity. The stress ratio can be computed based on the information given by the Mohr's circle representation as $\sigma_x / (\lambda \sigma_x) = 5.94/8.37 = 0.71$. The stress capacity and demand of the longitudinal reinforcing steel entering nodal zone *F* are 0.75(420) = 315 MPa and 0.71(315) = 224 MPa, respectively.

5. Conclusions

The method described in this paper allows capacity assessment of nodal zones of any shapes, which are normally formed by the intersections of the effective widths of struts and ties framing into the nodes. The stress distribution is based on construction of discontinuous stress fields and can be determined based on consideration of equilibrium only, thus consistent with the strut-and-tie methodology. Different assumptions to account the force effects of ties on nodal zones are also possible.

The viability of this method has been shown through its implementation into a computer-based STM tool CAST and through calculation examples. It is recognized that the geometry involved makes it essential to use a computer-based STM. However, it is well recognized that the application of STM for strength design is usually complicated by the need to perform iterative and time-consuming calculations and involves extensive graphical representations of strut-and-tie models (Tjhin and Kuchma 2002). As a result, computer-based STM tools equipped with graphics, analysis, and design tools, such as CAST, become essential to enable the designer to focus on the selection and design of the idealized load-resisting trusses.

Acknowledgments

Association, and the National Science Foundation.

References

ACI Committee 318 (2005), *Building code requirements for structural concrete (ACI 318-05) and commentary (ACI 318R-05)*, American Concrete Institute, Farmington Hills, MI.

Alshegeir, A. and Ramirez, J. A. (1992), "Computer graphics in detailing strut-tie models", *J. Comp. in Civ. Eng.*, **6**(2), 220-232.

Bergmeister, K., Breen, J. E. and Jirsa, J. O. (1991), "Dimensioning of nodal zones and anchorage of reinforcement", *IABSE Colloquium Stuttgart 1991: Structural Concrete*, International Association for Bridge and Structural Engineering, Zürich, Switzerland, 551-564.

Chen, W. F. and Drucker, D. C. (1969), "Bearing capacity of concrete blocks or rock", *J. Eng. Mech. Div.*, ASCE, **95**(4), 955-978.

Chen, W. F. and Han, D. J. (1988), *Plasticity for Structural Engineers*, Springer-Verlag, Inc., New York, NY.

Hadley, G. (1962), *Linear Programming*, Addison-Wesley Publishing Company, Inc., Reading, MA.

Hajdin, R. (1990), "Computerunterstützte berechnung von stahlbetonscheiben mit spannungsfeldern", *Report No. 175*, Institut für Baustatik und Konstruktion, Eidgenössische Technische Hochschule, Zürich, Switzerland.

Marti, P. (1985), "Basic tools of reinforced concrete beam design", *ACI J., Proceedings*, **82**(1), 45-56.

Müller, P. (1978), "Plastische berechnung von stahlbetonscheiben und–balken", *Report No. 83*, Institut für Baustatik und Konstruktion, Eidgenössische Technische Hochschule, Zürich, Switzerland.

Nielsen, M. P. (1999), *Limit Analysis and Concrete Plasticity*, 2nd Ed., CRC Press LLC, Boca Raton, FL.

Schlaich, J., Schäfer, K. and Jennewein, M. (1987), "Toward a consistent design of structural concrete", *PCI J.*, **32**(3), 74-150.

Schlaich, M. and Anagnostou, G. (1990), "Stress fields for nodes of strut-and-tie model", *J. Struct. Eng.*, ASCE, **116**(1), 13-23.

Thompson, M. K., Ziehl, M. J., Jirsa, J. O. and Breen, J. E. (2005), "CCT nodes anchored by headed bars - part 1: behavior of nodes", *ACI Struct. J.*, **102**(6), 808-815.

Thompson, M. K., Jirsa, J. O. and Breen, J. E. (2006), "CCT nodes anchored by headed bars - part 2: capacity of nodes", *ACI Struct. J.*, **103**(1), 65-73.

Tjhin, T. N. (2004), "Analysis and design tools for structural concrete using strut-and-tie models", Ph.D. Thesis, University of Illinois at Urbana-Champaign, Urbana, IL.

Tjhin, T. N. and Kuchma, D. A. (2002), "Computer-based tools for design by the strut-and-tie method: advances and challenges", *ACI Struct. J.*, **99**(5), 586-594.

Tjhin, T. N. and Kuchma, D. A. (2004), *CAST – Computer-Aided Strut-and-Tie – Program, Report, and User's Manual (Version 0.9.11)*, University of Illinois at Urbana-Champaign, Urbana, IL. Available: www.cee.uiuc. edu/kuchma/strut_and_tie.

Tjhin, T. N. and Kuchma, D. A. (2007), "Integrated analysis and design tool for the strut-and-tie method", *Eng. Struct.* (in press, available online 30 March 2007).

Yun, Y. M. and Ramirez, J. A. (1996), "Strength of struts and nodes in strut-tie model", *J. Struct. Eng.*, ASCE, **122**(1), 20-29.

CM